


RESEARCH

Open Access



MoSey1 regulates the unfolded protein response, appressorium development, and pathogenicity of *Magnaporthe oryzae*

Zifeng Yang^{1†}, Meiqin Li^{1,2†}, Linwan Huang¹, Xinru Chen¹, Shuning Weng¹, Biregeya Jules¹, Abah Felix¹, Huakun Zheng¹, Xiaofeng Chen^{1,3}, Jun Zhang¹, Zonghua Wang^{1,3}, Yingying Cai^{4*}, Jingang Liang^{5*} and Wei Tang^{1,4*} 

Abstract

Endoplasmic reticulum (ER) is an enclosed three-dimensional eukaryotic membrane network composed of flattened sacs. Fusion of homologous membranes to the ER membrane is essential for the maintenance of this network structure. In yeast, ER membrane fusion is mediated by Sey1p, whose paralogues function distinctly in different species. In this study, we investigated the biological functions of *MoSEY1* in the devastating rice blast fungus *Magnaporthe oryzae* by functional genomic approach. Compared to wild type, deletion of *MoSEY1* considerably decreased the growth and conidia production of *M. oryzae*. Additionally, the absence of *MoSEY1* delayed appressorium formation and invasive hyphae growth. The appressorium function was also impaired in Δ *Mosey1* mutant. Subcellular localization analysis revealed that MoSey1 is localized at the ER. The Δ *Mosey1* mutant showed augmented sensitivity to ER stress. Additionally, we found that MoSey1 regulated the unfolded protein response, autophagy, and protein secretion in *M. oryzae*. In conclusion, our study unveiled the involvement of MoSey1 in the development, pathogenesis, and ER functions in *M. oryzae*.

Keywords Endoplasmic reticulum, *Magnaporthe oryzae*, Pathogenicity, Protein secretion, MoSey1

[†]Zifeng Yang and Meiqin Li contributed equally to this work.

*Correspondence:

Yingying Cai
Caiyy@zaac.ac.cn
Jingang Liang
liangjingang@agri.gov.cn
Wei Tang
tangw@fafu.edu.cn

¹ State Key Laboratory of Ecological Pest Control for Fujian and Taiwan Crops, College of Plant Protection, Fujian Agriculture and Forestry University, Fuzhou 350002, China

² Modern Agriculture Industrial Park Service Center, Agriculture and Rural Bureau of Wangjiang County, Anqing, Anhui 246200, China

³ Marine and Agricultural Biotechnology Laboratory, Institute of Oceanography, Minjiang University, Fuzhou 350108, China

⁴ State Key Laboratory for Managing Biotic and Chemical Threats to the Quality and Safety of Agro-Products, Institute of Plant Protection and Microbiology, Zhejiang Academy of Agricultural Sciences, Hangzhou 310021, China

⁵ Development Center of Science and Technology, Ministry of Agriculture and Rural Affairs, Beijing 100176, China



Background

The endoplasmic reticulum (ER) plays a central role in protein synthesis and secretion, which constitutes the largest endomembrane system in eukaryotic cells (Khaminets et al. 2015). Serving as a factory for protein processes, ER employs stringent quality control to effectively process proteins. Misfolded proteins are subjected to ER-associated degradation (ERAD), which degrades the targeted proteins to peptides via 26 S proteasome (Tang et al. 2020). The ERAD system primarily consists of chaperones, the 26S proteasome, ubiquitin-related enzymes, and auxiliary proteins. Several human diseases, such as Alzheimer's and Parkinson's diseases, have been linked to ERAD (Kaneko 2016; Qi et al. 2017). A previous study in the rice blast fungus *Magnaporthe oryzae* implicates that the ubiquitin ligase MoHrd1 and the ER transmembrane protein MoDer1 regulate ERAD, and they are crucial for ER stress tolerance, protein secretion, and autophagy (Tang et al. 2020). The study showed that simultaneously knocking out of *MoHRD1* and *MoDER1* resulted in the abolishment of pathogenicity in *M. oryzae* (Tang et al. 2020). Accumulation of unfolded or misfolded proteins in the ER lumen disrupts ER protein homeostasis, leading to ER stress. This stress stimulates the unfolded protein response (UPR), which transmits signals to the nucleus and subsequently increases protein folding capacity in the ER. In *M. oryzae*, the mRNA of *MoHAC1*, encoding a transcription factor bZIP, undergoes specific shearing, leading to the entry of active Hac1 protein into the nucleus. This process regulates the expression of related target genes, enhancing protein folding capacity and relieving ER stress (Tang et al. 2015; Xia, 2019).

Recent studies indicate that if the ER is not sufficiently relieved from prolonged stress, selective autophagy would occur in the cells. Organisms may bundle aged or damaged organelles and proteins and deliver them to specific organelles (lysosomes in animals or vacuoles in plants and fungi) for degradation (Kershaw and Talbot 2009; Deng et al. 2012; Kania et al. 2015). Autophagy of the ER is crucial for diminishing stress and maintaining ER homeostasis. Autophagy comprises vesicle delivery, macroautophagy and microautophagy, with macroautophagy being the major area of researches nowadays (Loi et al. 2019; Smith and Wilkinson 2017).

Sey1 protein belongs to the dynamin superfamily proteins (DSPs) and presents in all eukaryotes with diverse biological functions in various organs or organelles. At11/2/3 are mammalian homologues of Sey1. *ATL1* is involved in the formation of ER vesicles, and *ATL2* functions downstream of *FAM134B*, a mouse ER-phage receptor (Liang et al. 2018). Overexpression of *FAM134B* in *ATL2* deletion mutants impedes the levels of ER autophagy. Furthermore, *ATL3* specifically binds

to autophagosomes and promotes the degradation of tubular ER during starvation (Liang et al. 2018; Jiang et al. 2020). In yeast, Sey1 is involved in the fusion of membranes with ER, and its absence delays or even prevents membrane fusion (Anwar et al. 2012). In *Dictyostelium discoideum*, deletion of *SEY1* leads to atypical ER architecture and the induction of protein degradation pathways, especially the UPR pathway. Furthermore, Sey1 impacts vesicle expansion (Hüsler et al. 2021). In *Arabidopsis*, deletion of *RHD3* results in stunted growth, curled root hairs, and impaired cell enlargement (Ueda et al. 2016; Zhang et al. 2013). In *Fusarium graminearum*, the absence of *FgSEY1* leads to decreased virulence and attenuated mycelial growth (Chong et al. 2020).

Rice blast, a fungal disease caused by *M. oryzae*, significantly and devastatingly impairs rice production worldwide. Given its economically important impact and established genetic manipulation system, *M. oryzae* has been selected as a model for the study of filamentous fungal phytopathogens. Although Sey1 has been studied in many organisms and found to play different roles in different species, its biological functions in *M. oryzae* remain unknown. The objective of this study is to unveil the biological roles of MoSey1 in *M. oryzae* and investigate its functions in this model phytopathogen.

Results

Identification and characterization of MoSEY1 in *M. oryzae*

MoSey1 protein sequence was obtained by BLASTp search using the *Saccharomyces cerevisiae* Sey1p sequence as a query. In addition, PFAM (<http://pfam-legacy.xfam.org/>) and PHYRE2 (<http://www.sbg.bio.ic.ac.uk/phyre2/>) were used for domain prediction and TBtools (<https://github.com/CJ-Chen/TBtools-II/releases>) was used for structure prediction. These analyses revealed that MoSey1 has five domains: GTPase domain, helix bundle domain, cytosolic tail domain, and two transmembrane segments (Additional file 1: Figure S1a). Furthermore, phylogenetic analysis revealed a close similarity between MoSey1 and Sey1 proteins in *F. graminearum* and *F. oxysporum* (Additional file 1: Figure S1b).

MoSey1 is involved in hyphae growth of *M. oryzae*

To investigate the biological roles of MoSey1 in *M. oryzae*, we deleted the *MoSEY1* gene and obtained Δ Mosey1 mutant (Additional file 1: Figure S2). *MoSEY1* was also reinserted into the mutant strain to obtain the Δ Mosey1/*MoSEY1* complemented strain. To examine the impact of *MoSEY1* on the growth of *M. oryzae*, the wide type (WT) Guy11, Δ Mosey1 mutant, and Δ Mosey1/*MoSEY1* complemented strain were cultured on complete media (CM), minimal media (MM), rice and corn media (SDC), and rice bran media (RBM) and incubated at 28°C under the

12 h/12 h light/dark photoperiod for 7 days. At the 7th day, we observed that the vegetative growth of $\Delta MoSEY1$ mutant on different media were significantly lower than those of the WT and complemented strains (Fig. 1a, b). To visualize and compare the aerial mycelia of various strains, the strains were grown on CM media side by side. The results showed that the colony of the mutant exhibited the smallest diameter (Fig. 1c).

Deletion of *MoSEY1* attenuates *M. oryzae* pathogenicity

To determine whether *MoSEY1* plays a role in the pathogenicity of *M. oryzae*, conidia from Guy11, $\Delta MoSEY1$ mutant strain, and the $\Delta MoSEY1/MoSEY1$ complemented strain were harvested and adjusted to same concentration (5×10^4 spores/mL). Equal volumes of the conidia suspensions were sprayed or punch inoculated onto 2-week-old rice leaves. The conidia were also injected into rice leaf sheaths. In addition, the conidia were dropped on barley leaves. The inoculated leaves were observed for disease symptoms at 7 days post inoculation (dpi). Only a few disease lesions were observed in the seedlings that were sprayed with the conidia suspension from the mutant strain, demonstrating a significantly reduced pathogenicity of the mutant compared to the WT and complemented strains (Fig. 2a, b). Similar disease symptoms were observed for the punch inoculation (Fig. 2c, d), rice leaf sheath injection, and barley leaves infection assays (Additional file 1: Figure S3a, b). Furthermore, we found that the number of conidia produced by the $\Delta MoSEY1$ mutant was significantly ($P < 0.01$) less than those of the WT and complemented strain (Additional

file 1: Figure S4a, b). These results indicate that *MoSEY1* plays an important role in the pathogenesis of *M. oryzae*.

To investigate the pathogenicity loss of $\Delta MoSEY1$ mutant strain, we inoculated rice sheaths with the spore suspensions of corresponding strains. The result showed that, at 24 hpi, about 80% of invasive hyphae from the WT expanded smoothly, whereas about 80% of spores from $\Delta MoSEY1$ mutant only formed penetration peg. In contrast with the WT and complementation strain, whose invasive hyphae spread to the secondary cell at 36 hpi, the invasive hyphae of $\Delta MoSEY1$ were exclusively constrained in the first-infected cell (Fig. 2e, f). Similar phenomena were observed in barley epidermal cells that were infected with the strains at 48 hpi (Additional file 1: Figure S5). These findings suggest that *MoSEY1* plays an important role in host colonization of *M. oryzae*.

***MoSEY1* regulates appressorium formation and functions**

In attempt to explain the reduced pathogenicity of $\Delta MoSEY1$ mutant, spores from WT, $\Delta MoSEY1$ mutant, and the complemented strains were inoculated on artificial hydrophobic surfaces. After 4 h of incubation, we observed that the spores of WT and the complemented strains had germinated and formed appressoria at the tips of the germ tubes, while the $\Delta MoSEY1$ mutant could not form appressoria until 6 h of incubation (Fig. 3). However, at 10 h of incubation, the $\Delta MoSEY1$ mutant formed appressoria similar to those of the WT and complemented strain.

The level of turgor pressure generated in an appressorium determines the strength of the blast fungus to

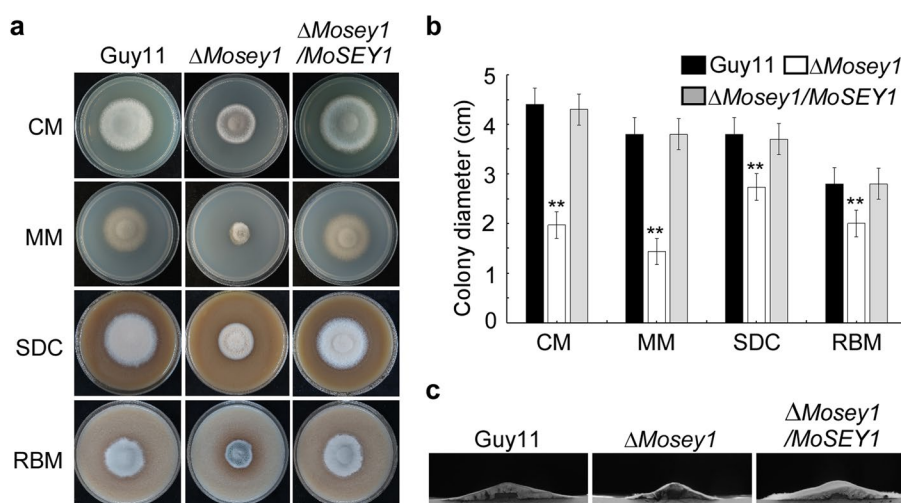


Fig. 1 Role of *MoSEY1* in *M. oryzae* vegetative growth. **a, b** Absence of *MoSEY1* gene causes a significant reduction in the vegetative growth of $\Delta MoSEY1$ mutant. The Guy11, $\Delta MoSEY1$ mutant, and complemented strains were cultured on different media at 28°C for a week. Values are presented as means \pm SD (standard deviation) calculated from three independent experiments. Double asterisks denote significant difference at $P < 0.01$ ($n = 2$). **c** Lateral view of the colonies of the indicated strains. After growth on CM agar for one week, each of the colonies was cut into two equal halves and viewed laterally. CM: complete medium; MM: minimal medium; SDC: rice and corn media; RBM: rice bran media

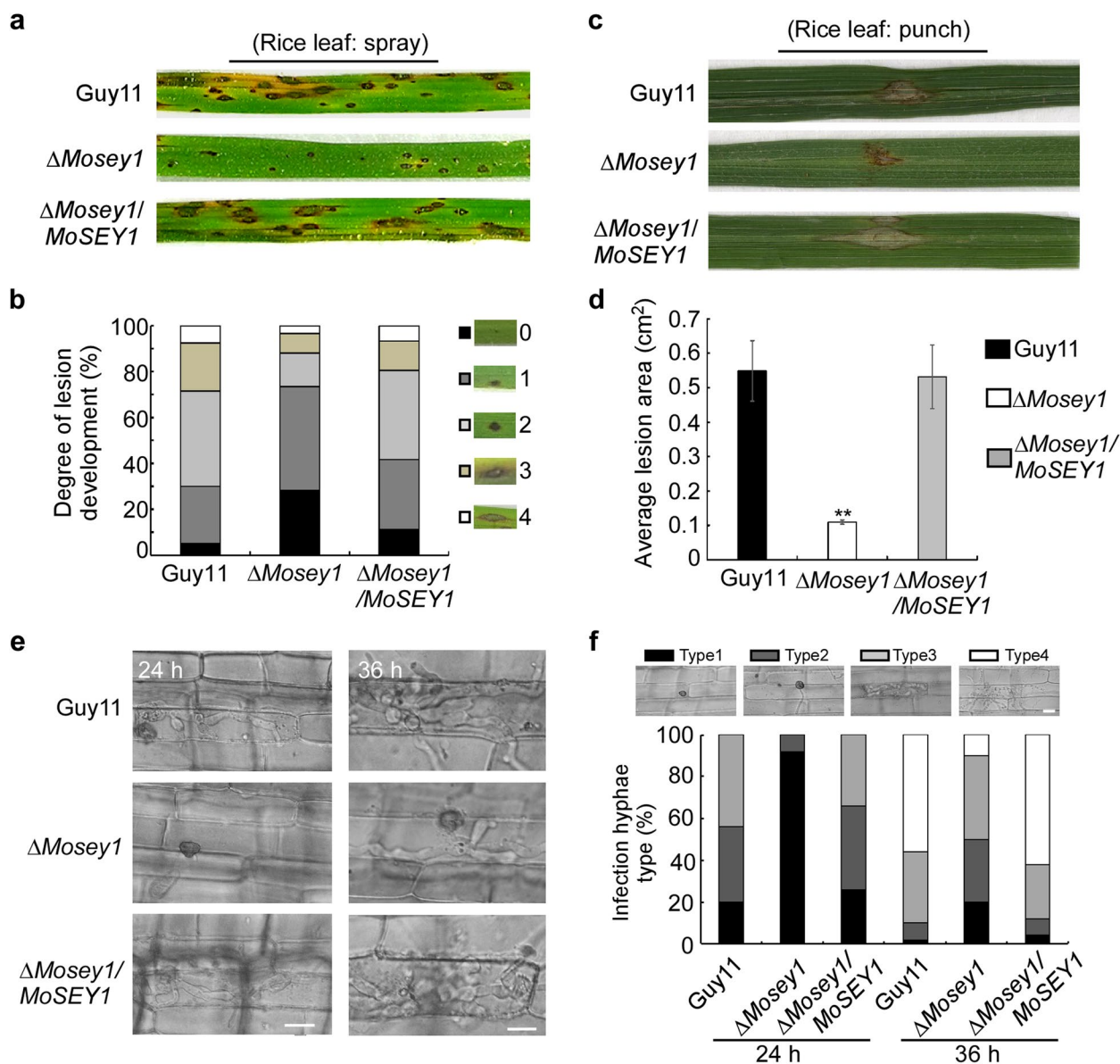


Fig. 2 Contribution of MoSeY1 to the pathogenicity of *M. oryzae*. **a, b** Spray inoculation assays on rice seedlings. **c, d** Punch inoculation assays on 2-week-old rice leaves. The lesions were measured. **e** Excised rice sheath from 4-week-old rice seedlings were inoculated with conidia suspension. Invasive hyphae were observed at 24 and 36 h. Scale bars: 10 μ m. **f** Statistical analysis for invasive hyphal growth in rice leaf sheaths at 24 and 36 hpi. Scale bars: 10 μ m. Values are presented as means \pm SD, calculated from three independent experiments. Double asterisks denote significant difference at $P < 0.01$ ($n = 2$)

penetrate its host. To further investigate whether the reduced pathogenicity of the Δ Mosey1 mutant strain was due to a defect in appressorium turgor generation, we measured the levels of turgor pressure generated in the appressoria of the various strains by cytorrhysis assay. The results showed that at 24 h of treatment with glycerol, the appressoria collapse rate of the Δ Mosey1 mutant was significantly higher than that of the WT when treated with low concentrations of glycerol (1 M, 2 M, and 3 M),

indicating that the turgor pressure in the Δ Mosey1 mutant appressoria was significantly reduced (Additional file 1: Figure S6a). However, when treated with high glycerol concentrations, the appressoria collapse rate of the Δ Mosey1 mutant was similar to that of the WT and the complementation strains. Different concentrations of PEG3350 (25%, 30%, 35%, and 40%) were used to further measure the appressorium turgor pressure of different strains, in which similar results were obtained to those in

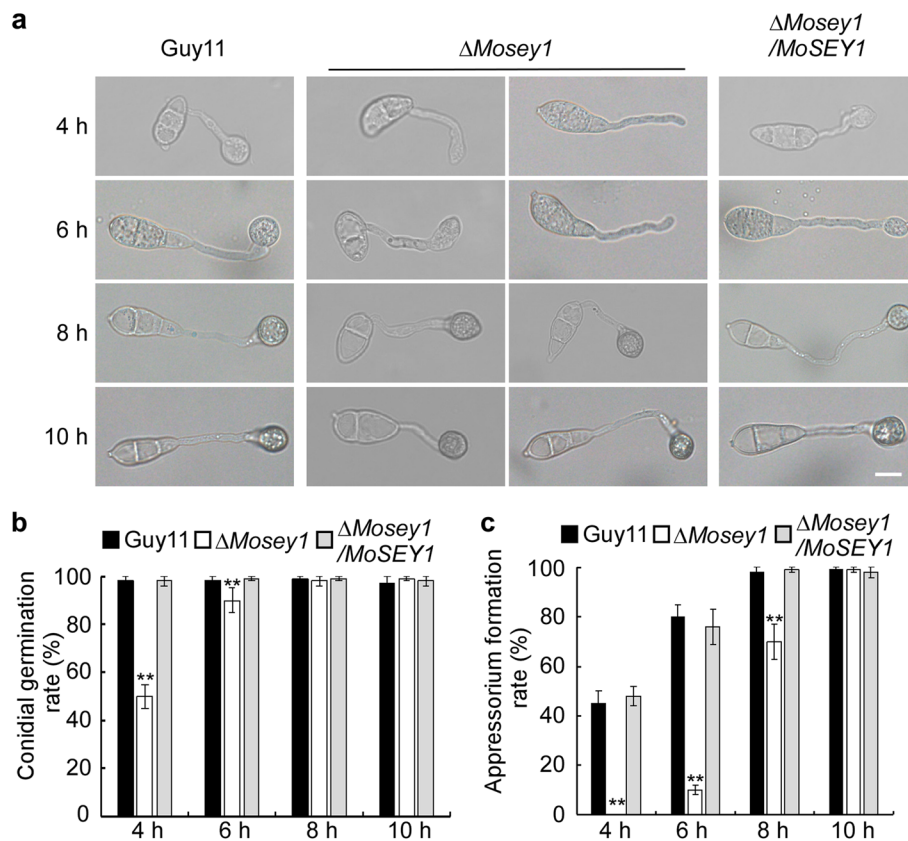


Fig. 3 Conidia germination and appressoria formation of different strains. **a** Conidia germination and appressoria formation on hydrophobic coverslips at different time points. Scale Bars: 10 μ m. **b** Analysis of the rates of conidia germination of the strains on artificial hydrophobic surfaces at the indicated time points. Values are presented as means \pm SD calculated from three independent experiments. **c** Analysis of the rates of appressoria formation of the indicated strains on artificial hydrophobic surfaces at the indicated time points. Values are presented as means \pm SD, calculated from three independent experiments. Double asterisks denote significant difference at $P < 0.01$

glycerol treatments (Additional file 1: Figure S6b). These results suggest that *MoSEY1* is involved in appressoria turgor generation in *M. oryzae*.

Mobilization and utilization of glycogen and lipids are required for appressorium formation in *M. oryzae* (Wang et al. 2007; Yan et al. 2013). To investigate whether *MoSEY1* plays any role in nutrient mobilization and utilization during conidia germination and appressorium formation, we carried out iodine/potassium iodide (I_2/KI) staining to monitor glycogen transport and metabolism during these processes. The results showed that glycogen was largely produced and utilized in spores and appressoria by the WT and the complemented strain within 48 h of incubation. In $\Delta Mosey1$ mutant, although glycogen was produced normally in conidia and appressoria as observed in the controls, the stained glycogen remained undegraded in both the conidia and appressoria of the mutant at 48 h of incubation (Fig. 4a, c), suggesting that deletion of *MoSEY1* perturbs glycogen utilization. In addition, we used the lipid-specific stain, Bodipy, to stain and analyze lipid mobilization and utilization during

spore germination and appressorium formation. At early stage, all the strains stained with Bodipy showed green fluorescence under GFP fluorescence excitation. Following the development of appressoria, lipid droplets were translocated from spores to appressoria within 24 h of incubation in the WT. However, the mutant strain still lacked lipid droplets in the appressoria. After 48 h of incubation, the lipid droplets in WT appressoria were largely consumed, and only little green fluorescence was seen, whereas the mutant spores and appressoria still showed strong green fluorescence (Fig. 4b, d). Taken together, these results suggest that $\Delta Mosey1$ mutant has reduced appressorium turgor pressure, delayed appressorium formation, impaired glycogen utilization, and perturbed translocation and utilization of liposomes in the appressoria.

MoSeY1 is localized to the ER in *M. oryzae*

To gain further insights into the functions of MoSeY1 in *M. oryzae*, we investigated the subcellular localization of the protein in *M. oryzae* strain expressing MoSeY1-GFP.

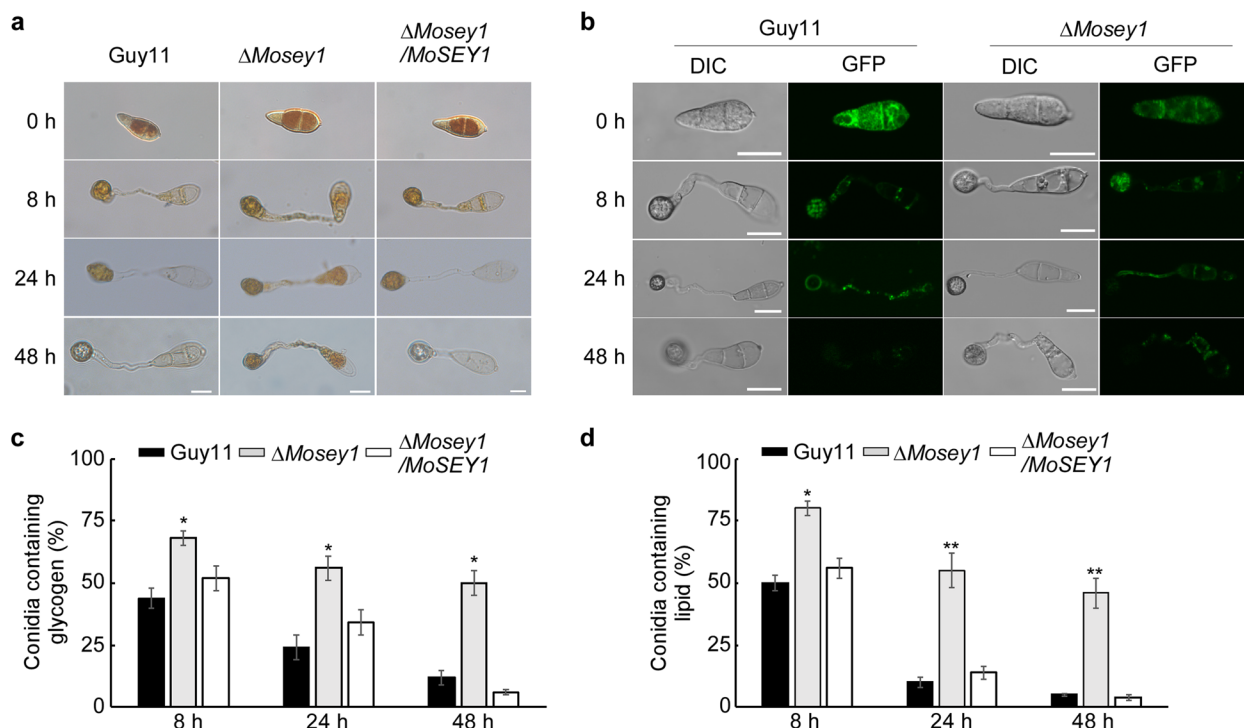


Fig. 4 Roles of *MoSEY1* in the utilization of glycogen and lipid droplets in appressoria. **a** Conidia were stained with I₂/KI for detection of glycogen translocation and degradation. **b** GFP-expressing conidia were stained with Bodipy for detection of lipid translocation and degradation. Scale bars: 10 μm. **c, d** Statistical analysis of glycogen and lipid transfer rate during conidia germination of *Guy11*, Δ *Mosey1* mutant, and complemented strains. Values are presented as means \pm SD, calculated from three independent experiments. Single asterisk denotes a significant difference at $P < 0.05$. Double asterisks denote a significant difference at $P < 0.01$ ($n = 2$)

Because this protein has been reported to localize to the ER in yeast, we co-expressed *MoSey1*-GFP with RFP-*MoLhs1*, an ER marker protein, for co-localization analysis. The results showed that *MoSey1* was expressed in conidia, mycelia, appressoria, and invasive hyphae, and the GFP and RFP signals were co-localized in these fungal structures (Fig. 5a). This result indicates that *MoSey1* is localized in the ER.

***MoSEY1* is involved in the regulation of ER stress response**

It was reported that the *Sey1* protein mediates vesicle fusion with the ER in yeast, where it plays an indispensable role in ER functions (Anwar et al. 2012). Therefore, we decided to determine the effects of *MoSEY1* deletion on ER stress tolerance by inoculating mycelial blocks from WT, Δ *Mosey1* mutant, and the complemented strain Δ *Mosey1*/*MoSEY1* onto CM media plates supplemented with ER stress-inducing agents, 2 mM DTT (dithiothreitol) and 0.5 μg/mL TM (tunicamycin), respectively. After a week of incubation in the dark, we observed that the growth of the Δ *Mosey1* mutant was significantly reduced, and displayed an increased sensitivity to ER stress (Fig. 5b, c), indicating the involvement of *MoSEY1* in ER stress response.

The UPR signaling pathway is regarded as part of the ER stress response, in which the fungal *MoHAC1* gene serves as a transcription factor (TF) (Tang et al. 2020). The UPR signaling pathway flickers two bands, namely *MoHAC1*^S and *MoHAC1*^U, through the splicing of *MoHAC1* mRNA. By splicing itself, the gene undergoes a code-shifting mutation that terminates protein translation prematurely (Tang et al. 2020). To investigate whether *MoSEY1* mediates the UPR in *M. oryzae*, we first examined the splicing levels of *MoHAC1* mRNA. The proportion of *MoHAC1*^S/*(MoHAC1*^S + *MoHAC1*^U) was calculated for splicing levels. The results indicated that the ratios of spliced mRNA to total mRNA in WT and the complemented strain were 0.47 and 0.49, respectively, while the ratio in Δ *Mosey1* mutant strain was 0.29 (Fig. 5d). These findings suggest that the deletion of *MoSEY1* leads to a decreased *MoHAC1* mRNA splicing. Since *MoHac1* functions as a TF in the UPR and is important for the expression of UPR target genes (Tang et al. 2015), the expression levels of the target genes related to the UPR, namely ER misfolded protein transporters *MoSEC61*, *MoHAC1*, and ER molecular chaperone *MoKAR2*, were investigated. The result shows that the expression of *MoKAR2* gene was notably reduced in the Δ *Mosey1* mutant strain (Fig. 5e).

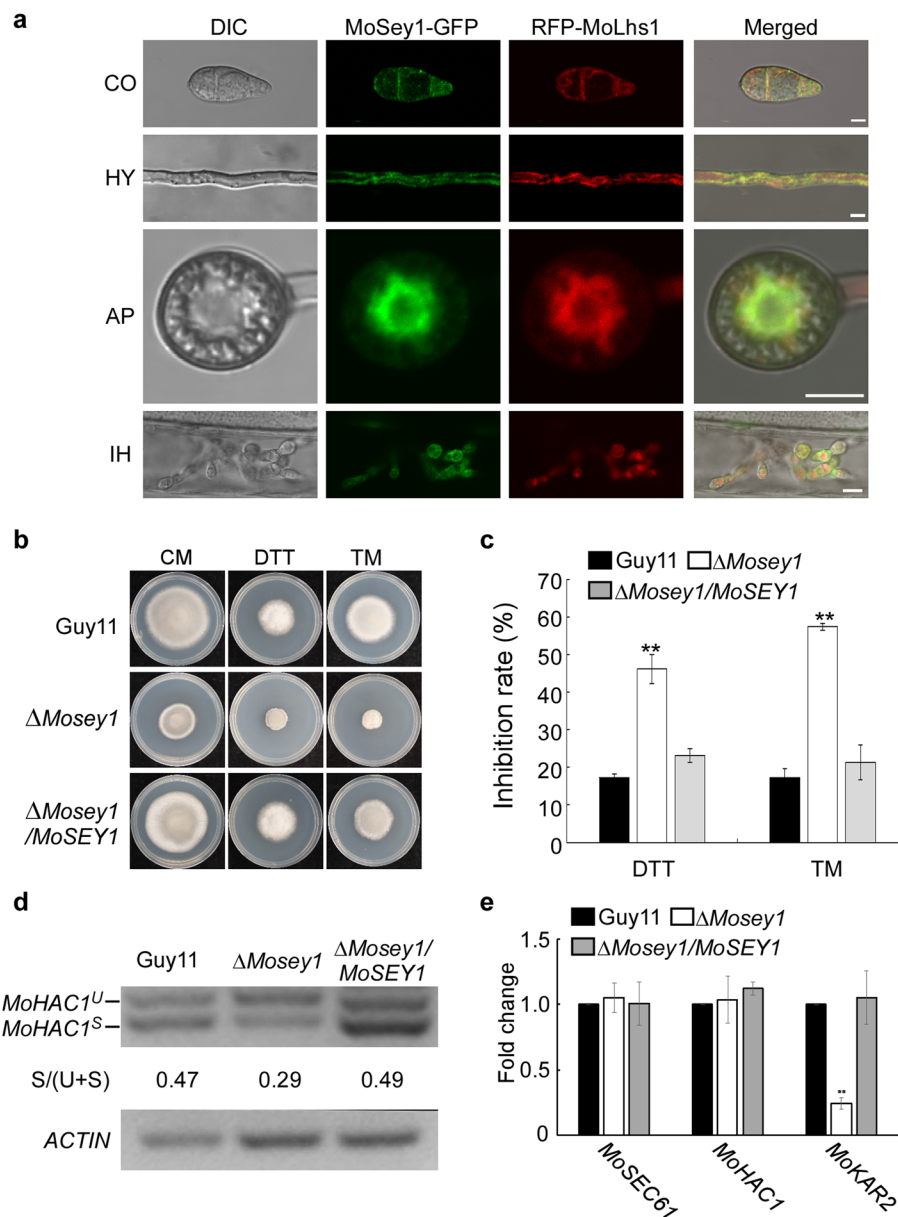


Fig. 5 MoSey1 regulates ER stress in *M. oryzae*. **a** MoSey1-GFP co-localizes with the ER marker RFP-MoLhs1 in conidia (CO), hyphae (HY), appressoria (AP), and invasive hyphae (IH). The strain co-expressing Sey1-GFP and RFP-MoLhs1 was visualized under a confocal microscope. Scale bars: 10 μm. **b, c** Vegetative growths and inhibition rates of the indicated strains on media supplemented with ER stress-inducing agents. **d** RT-PCR analysis for the UPR-induced splicing in different fungal strains. **e** Transcription levels of genes regulating the UPR pathway in *M. oryzae*. Values are presented as means ± SD, calculated from three independent experiments. Double asterisks denote significant differences at $P < 0.01$

These results indicate that *MoSEY1* mediates the UPR signaling pathway by modulating the unconventional splicing of the bZIP TF *MoHAC1* mRNA in *M. oryzae*.

MoSey1 is involved in protein secretion in the blast fungus

Our subcellular localization analysis showed that MoSey1 is situated in the ER, an organelle that is known for protein packaging and secretion. We therefore investigate

whether deleting of *MoSEY1* affects the protein secretion capability. Secreted proteins from WT and *ΔMosey1* mutant were separately extracted and analyzed by silver staining. The result revealed that the protein bands of *ΔMosey1* mutant were less intense than those of the WT (Fig. 6). Additionally, some bands in WT samples were completely absent in the mutant, which suggests that MoSey1 plays a role in the protein secretion in *M. oryzae*.

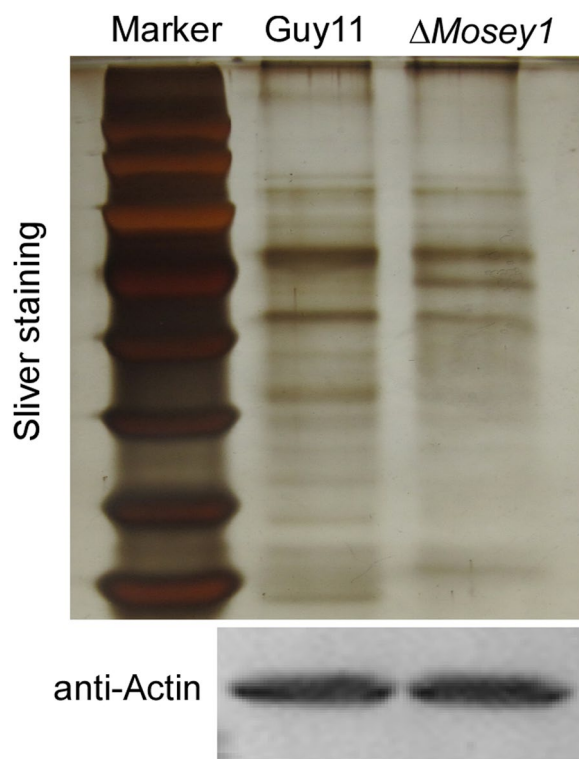


Fig. 6 The secreted proteins were reduced in $\Delta Mosey1$ mutant. SDS-PAGE analysis of Guy11 and $\Delta Mosey1$ secreted proteins. Silver staining is used to detect the protein bands after electrophoretic separation on polyacrylamide gels. Total proteins from the mycelia of Guy11 and $\Delta Mosey1$ were harvested and equalized using ACTIN as the internal reference

MoSEY1 regulates autophagy in *M. oryzae*

When prolonged ER stress is not relieved, cells will initiate autophagy. As such, we investigated whether MoSey1 takes part in the autophagic process. We induced ER stress in *M. oryzae* by expressing the GFP-tagged autophagy marker *GFP-MoATG8* in the WT and $\Delta Mosey1$ mutant strains, respectively. Autophagy was induced by culturing the strains in nitrogen-deficient minimal media (MM-N) for 4 h and then they were stained using CMAC dye. It showed that WT had considerably more green fluorescence in vesicles after induction, with 97% of the vesicles displaying fluorescence as opposed to the strain without autophagy induction. In $\Delta Mosey1$ mutant, the green fluorescence was only observed in about 20% of the vesicles, with majority of the fluorescence remaining dispersed throughout the cytoplasm (Fig. 7a, b). Using an electron microscopy, we observed that there were considerably fewer clustered autophagic vesicles in the mutant strain as compared to the WT (Fig. 7c). The degradation rate of GFP-Atg8 usually served as an index to measure the flux of autophagy. To determine the degree of autophagy at the protein level,

we expressed the GFP-MoAtg8 fusion protein in WT and $\Delta Mosey1$ mutant. Mycelia proteins of transgenic strains were extracted after inducing autophagy in liquid minimal medium with reduced nitrogen (MM-N) for 2 h and 4 h, respectively. Both the full-length GFP-MoAtg8 band (41 kDa) and the free GFP band (26 kDa) were detected in each stage. The proportion of GFP/(GFP + GFP-MoAtg8) was calculated for autophagic activity. The result shows that the levels of free GFP in the WT (from 44 to 53 to 61%) was higher than that in the mutant (from 47 to 51 to 55%) after induction of autophagy for 2 and 4 h, which indicates that MoSey1 contributes to autophagy (Fig. 7d). Therefore, we conclude that MoSey1 plays a crucial role in the autophagic process of *M. oryzae*.

Screening MoSey1 interacting proteins

To further uncover the function of MoSey1, we screened the candidate proteins that could interact with MoSey1 using GFP-conjugated beads to pull down MoSey1-GFP and its associated proteins in the $\Delta Mosey1/MoSEY1$ complemented strain. The Guy11 and Guy11-GFP (ectopically expressed GFP in Guy11) were used as negative controls. The candidate interacting proteins were identified by mass spectrometry (Fig. 8a), in which 33 potential MoSey1-interacting proteins were captured and identified (Fig. 8b). The analysis revealed that these candidate proteins are primarily involved in biological processes, such as protein translation, polypeptide biosynthesis, and ribosome biogenesis (Additional file 2: Table S1). To further explore the interacting proteins of MoSey1, we employed the yeast two-hybrid (Y2H) assay to confirm the interactions. Given that the N-terminal dynamin-related GTPase domain of Sey1 in yeast forms a dimer upon GTP binding (Praefcke and McMahon 2004), we initially focused on the investigation of the potential self-dimerization of MoSey1 in *M. oryzae*. The result suggests that MoSey1 is engaged in self-dimerization, implying that MoSey1 may exert its function through this self-dimerization (Additional file 1: Figure S7). However, the biological significance of MoSey1 interacting proteins remains to be investigated.

Discussion

ER is a highly dynamic organelle in eukaryotes. It is involved in protein modification, lipid synthesis, and regulation of Ca^{2+} signaling, among other functions (Anwar et al. 2012; Rogers et al. 2013). In *F. graminearum*, it is involved not only in the regulation of growth and pathogenicity, but also in the synthesis of lipid droplets and mycotoxins (Chong et al. 2020; Anwar et al. 2012). To investigate the biological function of MoSey1, we constructed the $\Delta Mosey1$ mutant strain. Biological function analysis revealed that MoSey1 is involved in regulating the vegetative growth of *M.*

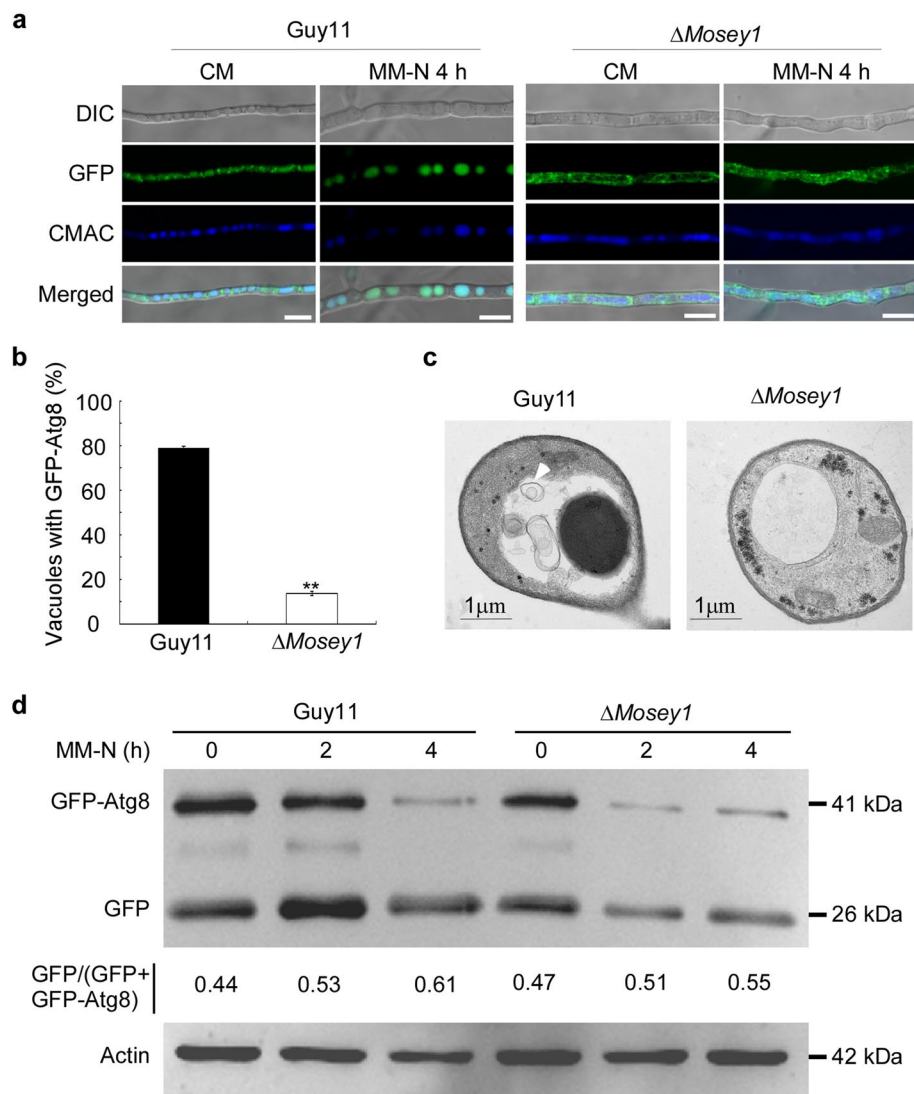


Fig. 7 Involvement of MoSey1 in autophagy. **a, b** Localization of GFP-MoAtg8 in $\Delta Mosey1$ mutant and wild type strains. The mycelia were cultured under 28°C for one day in CM liquid media, which then were washed with distilled water and transferred to MM-N liquid media containing 2 mM PMSF for 4 h. CMAC was used to stain the mycelia. Scale bars: 5 μ m. **c** Observation of organelles and autophagic bodies in hyphae cultured in MM-N for 4 h. Scale bars: 1 μ m. The arrow indicates an autophagic body. **d** Total mycelial proteins were extracted and analyzed after autophagy induction. The proteins were detected by western blot analysis with anti-GFP and anti-Actin antibodies. The flux of autophagy was estimated by calculating the amount of free GFP to GFP-Atg8. The band intensity was quantified by Image J software

oryzae. Through various pathogenicity analyses, it was found that the virulence of $\Delta Mosey1$ mutant decreased compared to the WT. Further microscopic examination of appressorium and invasive hyphae formation revealed that the $\Delta Mosey1$ mutant delayed the formation of appressorium and invasive hyphae. Additionally, the absence of *MoSEY1* gene affected turgor pressure of appressorium, transport of lipid droplets, and utilization of glycogen, suggesting that this may also contribute to the decrease in virulence.

In yeast, Sey1 is located at the ER and its absence impairs membrane fusion with the ER (Lee et al. 2015; Orso et al. 2009). In this study, it was found that MoSey1 also localizes at the ER. MoIre1 regulates ER unfolded protein signaling pathway and triggers variable shearing of the UPR response-related gene *MoHAC1*. This process impacts various functions including nutrient relocation and asexual reproduction in *M. oryzae* (Tang et al. 2015). Our study showed that *MoSEY1* gene could potentially participate in signaling pathways associated with the regulation of ER-associated protein homeostasis, since

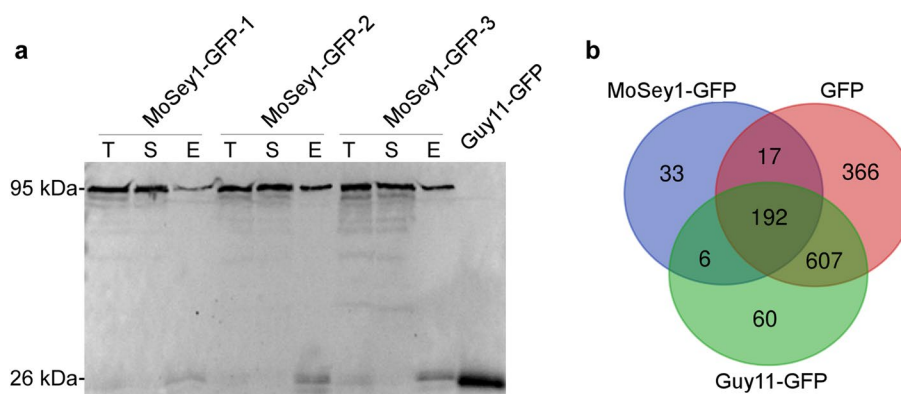


Fig. 8 Putative MoSey1-interacting proteins. **a** Western blot analysis for the expression of MoSey1-GFP. Total proteins were extracted from MoSey1-GFP expressing strains; T: total protein; S: protein suspension; E: eluted proteins from anti-GFP beads. **b** Venn diagram for MoSey1-GFP interacting proteins

deletion of *MoSEY1* gene resulted in decreased spliced levels of *MoHAC1* mRNA and a significant down-regulation of the expression of *MoKAR2* targeted UPR genes. It suggests that *MoSEY1* may impact ER-associated functions, which are in turn to adjust ER homeostasis. The conventional pathway of ER to Golgi is significant for protein secretion in *M. oryzae*. Importantly, the mutant exhibits a slight reduction in secreting proteins than the WT, revealing that *MoSEY1* affects the secretory capacity of *M. oryzae*. Many pathogens secrete effector proteins to suppress plant immunity at early stage of infection. In *M. oryzae*, the ER molecular chaperone MoLhs1 mediates the regulation of effector protein Avr-pita secretion (Yi et al. 2009). In this study, we identified several ER-associated proteins, such as MoYtn1 and MoYop1 (Additional file 2: Table S1), through mass spectrometry. We speculate that MoSey1 may also influence pathogenicity by modulating effector protein secretion through its interaction with ER-associated proteins.

During appressorium development, conidia transfer nutrients into the appressorium and facilitate the autophagic cell death of them. Lipid droplet transport is significantly reduced during autophagy, indicating the importance of autophagy in subsequent appressorium-assisted infection (Deng et al. 2012; Kershaw and Talbot 2009; Velázquez and Graef 2016). In yeast, *SEY1* affects physiological lipid droplet synthesis and size (Klemm et al. 2013). In our study, we found that some functions of the appressorium were affected in mutant when compared to the WT. This was evidenced by reduced turgor pressure and delayed glycogen and lipids translocations. Atlastin, a homologous of Sey1, has been reported as an ER-associated protein that serves as a component of the autophagosome. At12/3 can directly interact with Ulk1, a homolog of Atg1, to initiate autophagy. This interaction

promotes phagophore assembly on the ER, leading to autophagosome formation (Tang et al. 2020). In *M. oryzae*, autophagosome number can be determined by the amount of Atg8 present after shearing (Zhang and Xu 2014; Giraldo et al. 2013). In this study, our findings show that autophagosome initiation is reduced when subjected to nitrogen starvation. Additionally, electron microscopy observation confirmed that MoSey1 influences the process of autophagy. Our previous study shows that ER stress response is involved in the regulation of autophagy (Tang et al. 2020). Here, loss of Mosey1 disturbed the ER homeostasis and caused ER stress. We speculated that the defective autophagy in Δ *Mosey1* mutant may be caused by ER dysfunction. Further investigation will focus on exploring the function of MoSey1 in ER stress response and autophagy.

Conclusions

In this study, we identified MoSey1, a protein belonging to the dynamin superfamily, as a crucial factor in maintaining ER stability. Our findings revealed that the deletion of MoSey1 has an impact on protein secretion in *M. oryzae*. MoSey1 is also implicated in the regulation of signaling pathways and autophagy processes. Furthermore, our investigation reveals that MoSey1 plays a role in mediating appressorium function and is essential for the pathogenesis of *M. oryzae*. Consequently, our study unveils the connection between ER function and the fungal development as well as the virulence of *M. oryzae*.

Methods

Strains and culture conditions

In this study, the *M. oryzae* isolate Guy11 was used as the wild-type (WT) and, all other strains were generated from WT. All strains were cultivated on complete

medium (CM, 1 g yeast extract, 1 g casamino acid, 2 g peptone, 10 g D-glucose, 50 mL 20 × nitrate salts, 1 mL trace elements, 1 mL vitamin solution, 15 g agar, and distilled water added to a total volume of 1 L) agar plates. Mycelia were harvested from liquid CM for protoplast preparation, genomic DNA, RNA, and protein extractions. The fungal vegetative growth was tested on CM, minimal media (MM, 6 g NaNO₃, 0.52 g KCl, 0.152 g MgSO₄·7H₂O, 1.52 g KH₂PO₄, 0.01 g thiamine, 1 mL 1000 × trace elements, 10 g glucose, and 15 g agar and distilled water to 1 L), rice decoction & corn medium (SDC, 100 g of rice straw, 40 g of corn flour, and 15 g of agar in 1 L of distilled water) and rice bran media (RBM; 40 g of rice bran in 1 L of distilled water). All strains were cultured on SDC medium for Conidia production.

Bioinformatic analysis

The *Saccharomyces cerevisiae* Sey1 protein sequence was used as a query to search for its homolog (named MoSey1, MGG_06979) in *M. oryzae* genome at the FungiDB database (<https://fungidb.org/fungidb/app>). The Sey1 protein sequences of other fungi were obtained from the National Center for Biotechnology Information (NCBI) database (<https://www.ncbi.nlm.nih.gov/>) using the MoSey1 protein sequence as a query. Sequence alignment and phylogenetic analysis were performed using MEGA 6 software (Tamura et al. 2013). The phylogenetic tree was generated using the maximum likelihood method, with branches of the tree tested with 1000 bootstrap replicates.

Generation of gene deletion mutants and complementation strains

One-step gene replacement strategy was used to generate *MoSEY1* gene deletion mutant strain (Tang et al. 2015). Briefly, two 1.0 kb of homologous sequences upstream (A fragment) and downstream (B fragment) of the targeted gene were amplified, respectively, from Guy11 genomic DNA using their specific primer pairs (Additional file 2: Table S2). The hygromycin phosphotransferase (HPH) gene cassette was amplified from pCX62 plasmid using the HPH primer pairs (Additional file 2: Table S2). The A and B fragments were ligated with the HPH fragment at the upstream and downstream ends of the HPH, respectively, by splicing for overlap extension PCR (SOE-PCR). The SOE-PCR product was transformed into the WT protoplasts (Yu et al. 2004). Transformants were isolated from solid media containing hygromycin B drug (300 µg/mL). Six Δ *Mosey1* mutants were verified by PCR (Additional file 2: Table S2) and confirmed by Southern blot analysis. For complementation, the entire *MoSEY1* gene sequence plus its native promoter was amplified by PCR (Additional file 2: Table S2) and the resulted fragment was inserted into pYF11 vector, which was digested with

Xho I restriction enzymes, to obtain *MoSEY1-GFP* fusion construct. The construct was transformed into Δ *Mosey1* mutant protoplasts. Positive transformants were identified by PCR and was confirmed by GFP signal detection using a laser confocal microscope (Nikon, Japan).

Pathogenicity of *M. oryzae* and plant leaf infection assays

Plant infection assays were performed as previously described (Zhang and Xu 2014). Conidia suspensions from various strains were sprayed onto 2-week-old rice (*Oryza sativa* cv. CO39) seedlings or injected into rice sheaths at a concentration of 5×10^4 spores/mL in 0.2% (w/v) gelatin solution. The infected plants were observed for lesion development at 7 dpi. Lesions were divided into five levels: Level 0, no visible evidence of infection; Level 1, Brown lesions, the length is approximately 1 mm; Level 2, Small eyespot lesions, the length is approximately 2 mm; Level 3, Intermediate size lesions, the length is approximately 3–4 mm; Level 4, Large lesions, the length is more than 5 mm. For barley leaf inoculation assay, the 7-day-old barley leaves were cut and placed on moist filter papers in 15 cm Petri dishes. About 20 µL of conidia suspension (5×10^4 spores per mL) from various strains were dropped on the barley leaves, respectively. The inoculated leaves were incubated at 28°C for 5 days, and the disease symptoms were observed and photographed. The same concentration of conidial suspension was injected into the rice sheaths and incubated at 28°C for 24 h and 36 h. The rice sheaths were observed and photographed under microscope. Plant leaf infection was divided into 4 types: Type 1, appressoria were formed but unable to form invasive hyphae; Type 2, appressoria were formed with a single invasive hypha; Type 3, appressoria were formed and displayed minimal invasive hyphal growth; Type 4, appressoria were formed with extensive invasive hyphal growth.

Cytorrhysis analysis

About 20 µL of conidia suspensions (5×10^4 spores/mL) from various fungal strains were placed on hydrophobic coverslips, respectively, and incubated in a dark and humid box for 24 h at 28°C. After 24 h of incubation, the water was carefully drained and replaced with equal volume of glycerol at concentrations ranging from 1 M to 4 M. Ten minutes later, the number of collapsed appressoria was counted. More than 100 appressoria were observed for each glycerol concentration. For the glyco-gen staining assay, the samples were stained with 60 mg/mL KI and 10 mg/mL I₂.

Quantification of secreted proteins

Mycelia from various fungal strains were cultured in liquid MM for 2 days at 28°C and the culture was shaken at 150 rpm. The cultures were filtered and the filtrates were centrifuged at 3500 × *g* for 10 min. The supernatants were further filtered through 0.45 μm membrane filters to eliminate suspended mycelia and other parts of the fungi. Prechilled (-20°C) acetone (four times the volume of the filtrate) was added to each filtrate and incubated for 60 min at -20°C to precipitate proteins. The contents were centrifuged at 12,000 *g* for 10 min. The supernatants were discarded and the protein pellets were dried and re-suspended in 1×PBS buffer and stored at -20 °C for subsequent experiments. Protein gel staining was carried out using a Protein Fast Silver Stain Kit (Beyotime, Shanghai, China) according to the manufacturer's instructions (Tang et al. 2020).

Protein extraction and mass spectrometry

Mycelia from Δ *Mosey1/SEY1* strain were cultured in liquid CM for 2 days at 28 °C and the culture was shaken at 150 rpm. The mycelia were filtered, washed with sterile ddH₂O and ground to fine powder and then transferred to 1 mL of lysis buffer (10 mM Tris-HCl pH7.5, 150 mM NaCl, 0.5mM EDTA, and 0.5% Nonidet P-40) containing 10 μL protease inhibitor cocktail (APEX-BIO, Houston, America) and 1mM PMSE. After lysis, the content was centrifuged at 12,000 *g* for 10 min at 4°C. The supernatant was collected and incubated with GFP magnetic beads at 4°C overnight. The beads were then collected and washed three times with phosphate buffer solution (PBS, 8.0 g NaCl, 0.2 g KCl, 1.44 g Na₂HPO₄, 0.24 g KH₂PO₄, and distilled water added to a total volume of 1 L, pH7.4). The proteins bound to the beads were eluted and quantified by immunoblotting and identified by mass spectrometry at the Genomics company, Shenzhen, China.

Quantitative real-time PCR

Total RNA was extracted from the mycelia of different fungal strains harvested from liquid CM cultures after incubation at 28°C for 2 days at 180 rpm using an Eastep Super total RNA extraction kit (Promega, America). Quantitative PCR was performed using the SYBR kit (Vazyme, Nanjing, China) with specific primers (Additional file 2: Table S2). *Actin* (MGG_03982) was used as an endogenous reference gene in this experiment. The gene relative expression levels were evaluated using the 2^{-ΔΔCT} method as previously reported (Zheng et al. 2018). All experiments were repeated three times for each sample.

Statistical analysis

The experimental data were calculated and processed using Excel 2019, and one-way ANOVA was performed using data processing system (DPS). Levels of significance were tested using Duncan's new complex polarity method at *P* < 0.01.

Abbreviations

AP	Appressoria
CAMC	7-amino-4-chloromethylcoumarin
CM	Complete media
CO	Conidia
Dpi	Days post inoculation
DSPs	Dynamamin superfamily proteins
DTT	Dithiothreitol
ER	Endoplasmic reticulum
ERAD	Endoplasmic reticulum-associated degradation
HPH	Hygromycin phosphotransferase
Hpi	Hours post inoculation
HY	Hyphae
IH	Invasive hyphae
MM	Minimal media
RBM	Rice bran media
SDC	Rice and corn media
TF	Transcription factor
TM	Tunicamycin
UPR	Unfolded protein response
WT	Wide type
Y2H	Yeast two-hybrid

Supplementary Information

The online version contains supplementary material available at <https://doi.org/10.1186/s42483-024-00253-w>.

Additional file 1: Figure S1. Domain architecture of MoSey1 and phylogenetic relationship of Sey1 homologs. **a** Schematic protein structure of MoSey1. **b** Phylogenetic analysis of Sey1 in different species. **Figure S2.** The confirmation of *MoSEY1* deletion in *M. oryzae*. **a** The HPH probe and restriction enzymes used for Southern blot hybridization. **b** The Southern blot analysis for Guy11 and the *MoSEY1* knockout mutant. **Figure S3.** Contribution of *MoSEY1* to the pathogenicity of *M. oryzae*. **a** The disease symptoms observed after rice leaf sheath injection assay. **b** Pathogenicity assays on barley leaves. **Figure S4.** Effects of *MoSEY1* deletion on conidiation of *M. oryzae*. **a** Conidiophore production in fungal strains grown on SDC media. The mutant produced scanty conidiophores bearing fewer conidia. **b** Analysis of the number of conidia produced by the indicated strains. Values are presented as means ± SD, calculated from three independent experiments. Double asterisks denote significant differences at *P* < 0.01. **Figure S5.** Involvement of *MoSEY1* in the invasive growth of *M. oryzae* in barley cells. **a** *M. oryzae* infectious hyphae in infected barley leaves. Scale bars: 10 mm. **b** One-week-old barley leaves were inoculated with conidia suspension (5 × 10⁴ spores/mL) and invasive hyphae were observed at 48 h post-inoculation. Scale bars: 10 mm. **c** Statistical analysis for each type of invasive hyphal growth observed in barley at 48 hpi. **Figure S6.** *MoSEY1* deletion affects appressorium functions. **a** Statistical analysis of appressorium turgor pressure under different glycerol concentrations. **b** Statistical analysis of appressorium turgor pressure under different PEG concentrations. Values are presented as means ± SD, calculated from three independent experiments. Double asterisks denote significant differences at *P* < 0.01. **Figure S7.** Self-interaction verification of MoSey1. Yeast two-hybrid verification of the self-interaction of MoSey1. The AD-MoSey1 and BD-MoSey1 plasmids were co-transformed into yeast cells and screened on synthetic dextrose media lacking Leu and Trp (SD-2). The resulting single colonies were serially diluted onto SD-2 and SD-4 (synthetic dextrose media lacking Ade, His, Leu, and Trp) for the observation of yeast cell growth. The yeast co-transformed with pGADT7-T + pGBKT7-53

was employed as a positive control, while the yeast co-transformed with pGADT7-T + pGBKT7-lam was used as a negative control.

Additional file 2: Table S1. Candidate MoSey1-GFP interacting proteins.
Table S2. Primers used in this study.

Acknowledgements

We are grateful to Prof. Min Guo and Xinli Gong from Anhui Agricultural University for their assistance in the autophagy-related experiments.

Authors' contributions

ZY, ML, and WT designed the research; ZY, ML, LH, XC, SW, BJ, and AF performed the experiments; ZY drafted the manuscript; YC, JL, and WT revised the manuscript; HZ, XC, JZ, and ZW supervised the project. All authors read and approved the final manuscript.

Funding

This work was supported by grants from the Natural Science Foundation of Fujian Province (2022J01129), Fujian Provincial Science and Technology Key Project (2022NZ030014), Central Guidance on Local Science and Technology Development Fund of Fujian Province (2022L3088), State Key Laboratory for Managing Biotic and Chemical Threats to the Quality and Safety of Agro-products (2021DG700024-KF202406), and Special Fund for Science and Technology Innovation of Fujian Agriculture and Forestry University (CXZX2019007G).

Availability of data and materials

The data that support the findings of this study are available from the corresponding author upon request.

Declarations

Ethics approval and consent to participate

Not applicable.

Consent for publication

Not applicable.

Competing interests

The authors declare that the research was conducted without any commercial or financial relationships that could be construed as a potential conflict of interest.

Received: 2 January 2024 Accepted: 3 April 2024

Published online: 11 July 2024

References

- Anwar K, Klemm RW, Condon A, et al. The dynamin-like GTPase Sey1p mediates homotypic ER fusion in *S. cerevisiae*. *J Cell Biol.* 2012;197:209–17.
- Chong X, Wang C, Wang Y, et al. The dynamin-like GTPase FgSey1 plays a critical role in fungal development and virulence in *Fusarium Graminearum*. *Appl Environ Microbiol.* 2020;86:e02720–02719.
- Deng Y, Qu Z, Naqvi NI. Role of macroautophagy in nutrient homeostasis during fungal development and pathogenesis. *Cells.* 2012; 449–63.
- Giraldo MC, Dagdas YF, Gupta YK, et al. Two distinct secretion systems facilitate tissue invasion by the rice blast fungus *Magnaporthe oryzae*. *Nat Commun.* 2013;4:1996.
- Hüsler D, Steiner B, Welin A, et al. Dictyostelium lacking the single atlastin homolog Sey1 shows aberrant ER architecture, proteolytic processes and expansion of the Legionella-containing vacuole. *Cell Microbiol.* 2021;23:e13318.
- Jiang X, Wang X, Ding X, et al. FAM134B oligomerization drives endoplasmic reticulum membrane scission for ER-phagy. *EMBO J.* 2020;39:e102608.
- Kaneko M. Physiological roles of ubiquitin ligases related to the endoplasmic reticulum. *Yakugaku Zasshi.* 2016;136:805–9.
- Kania E, Pająk B, Orzechowski A. Calcium homeostasis and er stress in control of autophagy in cancer cells. *Biomed Res Int.* 2015; 352794.
- Kershaw MJ, Talbot NJ. Genome-wide functional analysis reveals that infection-associated fungal autophagy is necessary for rice blast disease. *Proceedings of the National Academy of Sciences.* 2009; 106: 15967–15972.
- Khaminets A, Heinrich T, Mari M, et al. Regulation of endoplasmic reticulum turnover by selective autophagy. *Nature.* 2015;522:354–8.
- Klemm robin W, Norton justin P, Cole ronald A, et al. A conserved role for atlastin GTPases in regulating lipid droplet size. *Cell Rep.* 2013;3:1465–75.
- Lee M, Ko Y-J, Moon Y, et al. SNAREs support atlastin-mediated homotypic ER fusion in *Saccharomyces cerevisiae*. *J Cell Biol.* 2015;210:451–70.
- Liang JR, Lingeman E, Ahmed S, et al. Atlastins remodel the endoplasmic reticulum for selective autophagy. *J Cell Biol.* 2018;217:3354–67.
- Loi M, Raimondi A, Morone D, et al. ESCRT-III-driven piecemeal micro-ER-phagy remodels the ER during recovery from ER stress. *Nat Commun.* 2019;10:5058.
- Orso G, Pendin D, Liu S, et al. Homotypic fusion of ER membranes requires the dynamin-like GTPase atlastin. *Nature.* 2009;460:978–83.
- Praefcke GJK, McMahon HT. The dynamin superfamily: universal membrane tubulation and fission molecules? *Nat Rev Mol Cell Biol.* 2004;5:133–47.
- Qi L, Tsai B, Arvan P. New insights into the physiological role of endoplasmic reticulum-associated degradation. *Trends Cell Biol.* 2017;27:430–40.
- Rogers JV, Arlow T, Inkellis ER, et al. ER-associated SNAREs and Sey1p mediate nuclear fusion at two distinct steps during yeast mating. *Mol Biol Cell.* 2013;24:3896–908.
- Smith M, Wilkinson S. ER homeostasis and autophagy. *Essays Biochem.* 2017;61:625–35.
- Tamura K, Stecher G, Peterson D, et al. MEGA6: molecular evolutionary genetics analysis version 6.0. *Mol Biol Evol.* 2013;30:2725–9.
- Tang W, Ru Y, Hong L, et al. System-wide characterization of bZIP transcription factor proteins involved in infection-related morphogenesis of *Magnaporthe oryzae*. *Environ Microbiol.* 2015;17:1377–96.
- Tang W, Jiang H, Aron O, et al. Endoplasmic reticulum-associated degradation mediated by MoHrd1 and MoDer1 is pivotal for appressorium development and pathogenicity of *Magnaporthe oryzae*. *Environ Microbiol.* 2020;22:4953–73.
- Ueda H, Yokota E, Kuwata K, et al. Phosphorylation of the C terminus of RHD3 has a critical role in homotypic er membrane fusion in *Arabidopsis*. *Plant Physiol.* 2016;170:867–80.
- Velázquez AP, Graef M. Autophagy regulation depends on ER homeostasis controlled by lipid droplets. *Autophagy.* 2016;12:1409–10.
- Wang Z-Y, Soanes DM, Kershaw MJ, et al. Functional analysis of lipid metabolism in *Magnaporthe Grisea* reveals a requirement for peroxisomal fatty acid beta-oxidation during appressorium-mediated plant infection. *Mol plant-microbe Interactions: MPMI.* 2007;20:475–91.
- Xia X. Translation control of HAC1 by regulation of splicing in *Saccharomyces cerevisiae*. *International Journal of Molecular Sciences.* 2019.
- Yan X, Que Y, Wang H, et al. The MET13 methylenetetrahydrofolate reductase gene is essential for infection-related morphogenesis in the rice blast fungus *Magnaporthe oryzae*. *PLoS ONE.* 2013;8:e76914.
- Yi M, Chi M-H, Khang CH et al. The ER chaperone LHS1 is involved in asexual development and rice infection by the blast fungus *Magnaporthe oryzae*. *Plant Cell.* 2009;21: 681–95.
- Yu J-H, Hamari Z, Han K-H et al. 2004. Double-joint PCR: a PCR-based molecular tool for gene manipulations in filamentous fungi. *Fungal Genetics and Biology.* 2009; 41: 973–981.
- Zhang S, Xu J-R. Effectors and Effector Delivery in *Magnaporthe oryzae*. *PLoS Pathog.* 2014;10:e1003826.
- Zhang M, Wu F, Shi J, et al. Root hair defective3 family of dynamin-like GTPases mediates homotypic endoplasmic reticulum fusion and is essential for *Arabidopsis* development. *Plant Physiol.* 2013;163:713–20.
- Zheng H, Li L, Miao P, et al. FgSec2A, a guanine nucleotide exchange factor of FgRab8, is important for polarized growth, pathogenicity and deoxynivalenol production in *Fusarium Graminearum*. *Environ Microbiol.* 2018;20:3378–92.